Available online at www.sciencedirect.com
ScienceDirect
Journal of Power Sources 167 (2007) 391–397
JOURNAL OF POWER SOURCES
www.elsevier.com/locate/jpowsour

Current density measurements in direct methanol fuel cells

F. Ay [a], A. Ata [a], H. Dohle [b], T. Şener [c], H. Gorgun [d,*]

[a] *Gebze Institute of Technology, Material Science and Engineering Department, P.K. 141, 41400 Gebze, Kocaeli, Turkey*
[b] *Institut für Werkstoffe und Verfahren der Energietechnik (IWV-3), Forschungszentrum Jülich GmbH, D-52425 Julich, Germany*
[c] *TUBITAK, Marmara Research Center, Energy Institute, Kocaeli, Turkey*
[d] *Department of Electrical Engineering, Yildiz Technical University, 34349 Besiktas, Istanbul, Turkey*

Received 24 October 2005; received in revised form 31 January 2007; accepted 13 February 2007
Available online 25 February 2007

Abstract

The current density in the fuel cell is the direct consequence of reactions taking place over the active surface area. Thus, measurement of its distribution will lead to identification of the location and nature of reactions and will give opportunity to improve the overall efficiency of fuel cells. Within this study, the current density distribution in a direct methanol fuel cell was analyzed by segmenting the current collector into nine sections. Besides, the effect of the different operating parameters such as molarity, flow rate and reactant gas on the current density distribution was analyzed.

Keywords: Direct methanol fuel cell; Current density

1. Introduction

Direct methanol fuel cell (DMFC) is one of the most promising energy conversion devices for low-power applications ranging from laptops and cell phones to micro-electromechanical system (MEMS) devices. In DMFCs, methanol and water react to produce carbon dioxide, electrons and protons at the anode (Eq. (1)). The electrons and protons, which are transferred via external circuit and electrolyte membrane, respectively, react with oxygen to produce water at the cathode (Eq. (2)).

$$\text{Anode}: \quad CH_3OH + H_2O \rightarrow CO_2 + 6H^+ + 6e^- \tag{1}$$

$$\text{Cathode}: \quad \tfrac{3}{2}O_2 + 6H^+ + 6e^+ \rightarrow 3H_2O \tag{2}$$

$$\text{Total}: \quad CH_3OH + \tfrac{3}{2}O_2 \rightarrow 2H_2O + CO_2$$

The current density distribution is affected by stoichiometries of the fuel and oxidant (oxygen/air), humidification conditions, microstructure of the membrane electrode assembly and flow-field design. Uniform current distribution is essential to reduce the cost and to increase the performance of polymer exchange membrane type fuel cells for commercialization. The uniform current density provides maximum power densities as well as ensures maximum lifetime for the cell components whereas, poor current distribution results in poor reactant and catalyst utilization with a reduced overall energy efficiency, and increased corrosion processes in the cell.

It should be noted that both DMFC and PEMFC use PTFE-based membranes. Their operation temperature, current and power densities are similar. Thus, current distribution measurement techniques for PEMFCs could also be adopted and used for DMFC's [1,2].

In general there are three methods to determine the current density distribution in Polymer Electrolyte Membrane Fuel Cell (PEMFC); partial membrane electrode assembly technique [3], sub-cell technique [3] and current mapping [4–6].

The partial membrane electrode assembly (MEA) technique involves either masking different areas or partially catalyzing segments of the MEA to determine local current density behavior. The technique does not provide sufficient spatial resolution and significant errors might arise due to inherent variations in electrical, transport and kinetic properties between different MEAs.

The sub-cell technique involves a number of 'sub-cells' at various locations along the gas flow channel that were electri-

* Corresponding author. Tel.: +90 212259 7070x2657; fax: +90 212 259 4967.
E-mail addresses: ayfatih@gyte.edu.tr (F. Ay), gorgun@yildiz.edu.tr (H. Gorgun).

0378-7753/$ – see front matter © 2007 Elsevier B.V. All rights reserved.
doi:10.1016/j.jpowsour.2007.02.035

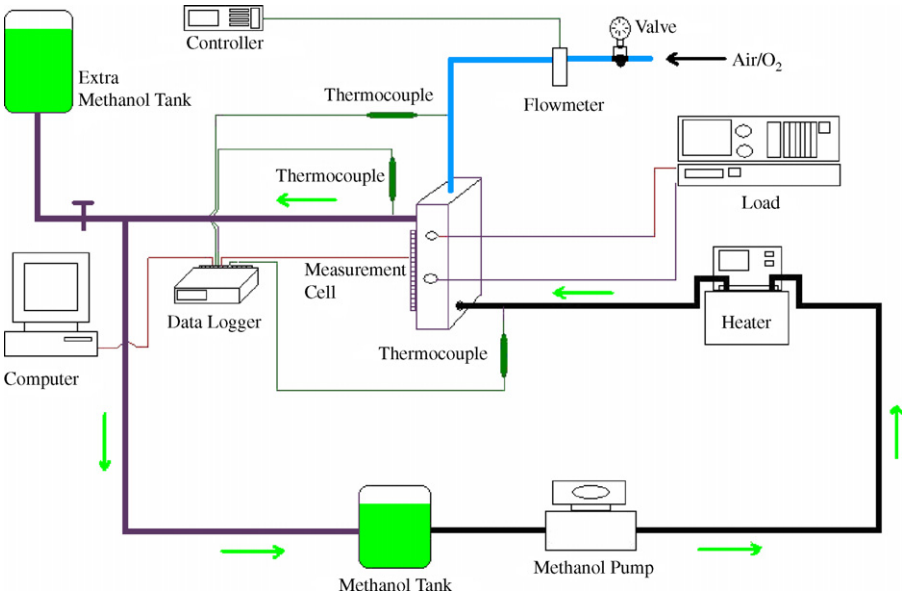

Fig. 1. Experimental set-up.

cally insulated from the main active MEA and controlled by a separate load. This technique is plagued by the difficulty in properly isolating the 'sub-cells' from the main electrode and achieving perfect alignment of the anode and cathode sides.

The current mapping technique involves a segmented current collector or segmented fuel cell component(s) (flow-field plate, GDL or MEA). Segmented current collector application has some variations in current collectors such as, printed circuit board as current collector [7] and conductive collector pieces in a non-conductive supporting structure such as polycarbonate [8], polysulfone [6,2].

The aim of the present work is to describe and demonstrate a technique for measurement of current density distribution in a DMFC using a segmented current collector supported on polysulfone plate and a standard, non-segmented MEA. The effect of the different operating parameters such as molarity, flow rate and reactant gas on the current density distribution was analyzed.

2. Experimental set-up

Fig. 1 illustrates the experimental set-up used during the study. The experiments were performed at 70 °C with home made MEA having 110 cm^2 active area. The membrane used was Nafion® 117, the catalysts were Pt–Ru (1:1) on the anode side and Pt-black on the cathode side with a loading of 2 mg cm^{-2}. A 1 M and 0.5 M methanol is supplied from the methanol tank through a peristaltic pump to the anode side. The methanol solution is also heated by a heater just before the test cell. An electronic load bank (Uniwatt Electronische Last EL 2000S) was used to operate at different current levels. All measurements are logged by Keithly Integra Series 2071 Ethernet Multimeter/data logger system.

Fig. 2 demonstrates the segmented current measurement cell used during the study. Separator and assembling plates are made up of stainless steel due to its high conductance and corrosion resistance to decrease current losses.

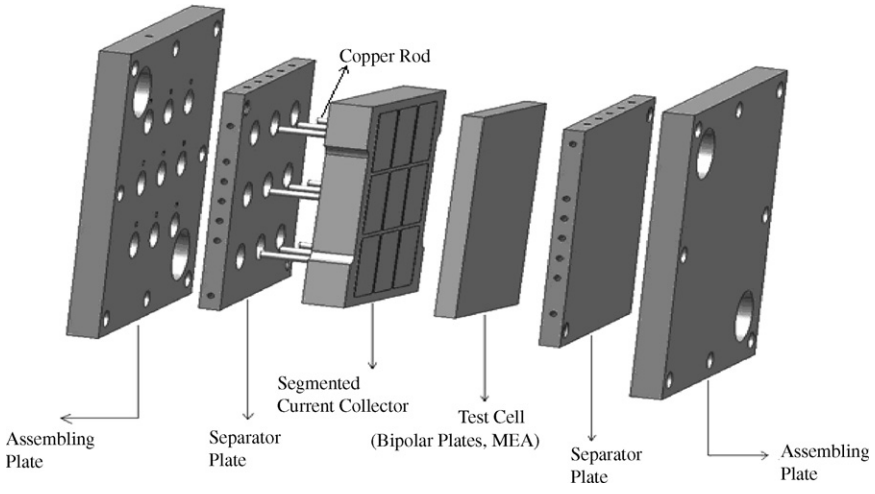

Fig. 2. Segmented cell.

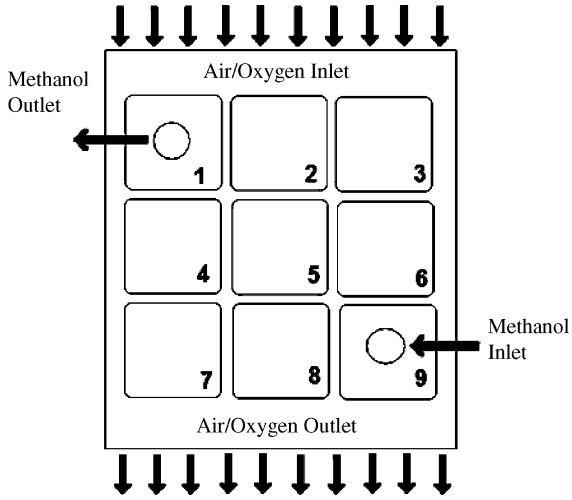

Fig. 3. Segments of measurement cell.

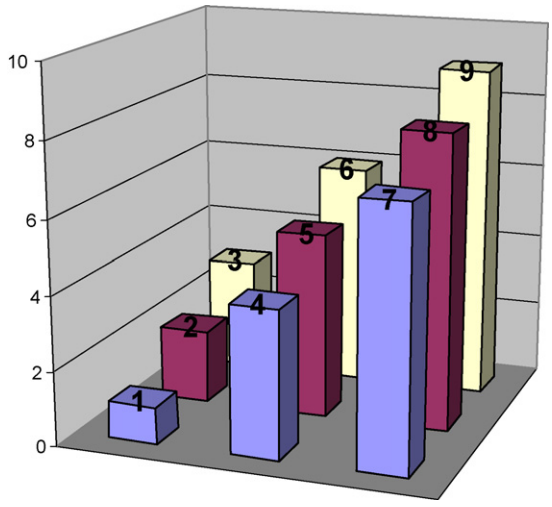

Fig. 4. Nine segments of current collector.

Support of segmented current collector is made up of polysulfone due to high temperature resistance and conductance. Nine copper-made and gold-coated current collector plates were placed in support partitions with a depth of 4 mm and with dimensions of 34 mm × 34 mm. Copper rods were attached to plates to make it possible to gather current data from outside of the measurement cell. Details of segments are presented in Fig. 3.

Copper wires were soldered to the ends of the copper rods extended from the segmented current collector through the outside of the measurement cell and these copper wires were used for the current density measurement. The resistance of the required wires must be in the range of 20–30 mΩ. The electronic load bank was simply used as a current supply to measure the resistance of each segment. The calculated resistance values for segment 1–9 are 0.0225, 0.0234, 0.0233, 0.0228, 0.0226, 0.0219, 0.0229, 0.0223 and 0.0247 Ω.

Oxidants (air/oxygen) were fed to the cell at a pressure of 3 bar and at a temperature of 24 °C. Operating temperature of the cell is 70 °C. It is important to point out that at every 3 h; methanol solution was changed to prevent any depletion in the methanol concentration during measurements. Before performing any measurement, it was awaited approximately 30–60 min for the stabilization of the cell. After 70 °C has been reached, desired current was drawn from the cell by increasing the current value slowly. The open circuit voltage of the test cell was between 500 and 700 mV and it is considered not to run the test cell at a voltage below 200 mV.

3. Results and discussion

Within this study, current distributions were observed under various operating conditions and comparative results are explored. At first experiments have been done with constant air flow rate but with variable methanol flow rates. Next, these experiments have been repeated using oxygen as oxidant instead air. Following, experiments have been done with constant methanol flow rate but with variable air flow rates. Finally, last experiments have been repeated using oxygen as oxidant instead air (Table 1).

3.1. Current density measurement at a constant air flow rate (13 l min^{-1}) by alternating methanol flow rate

The layout of the segments in the current density figures is given in Fig. 4. When 1 M Methanol was fed at a flow rate of 98 ml min^{-1} and 8 A current was withdrawn from the system, the current density distribution was as given in Fig. 5. Note that there is a significant difference between the current density values of segments. The maximum value was 90 mA cm^{-2}

Table 1
Numerical values for current density distribution figures

Figure	Segment 1	Segment 2	Segment 3	Segment 4	Segment 5	Segment 6	Segment 7	Segment 8	Segment 9
5	39	45	47	76	78	65	79	90	84
7	20	26	33	70	83	83	88	98	101
9	34	43	46	77	77	70	80	88	87
10	20	27	35	73	82	87	85	93	99
13	26	39	42	72	80	71	85	91	90
14	18	22	27	64	79	89	89	99	105
17	24	36	41	72	79	76	86	91	94
18	17	23	30	65	80	93	87	98	106

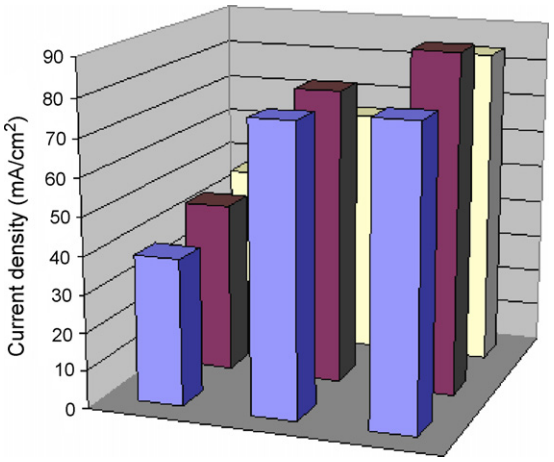

Fig. 5. Current density distribution for 98 ml min^{-1} 1 M methanol flow rate, 13 l min^{-1} air flow rate and 8 A current.

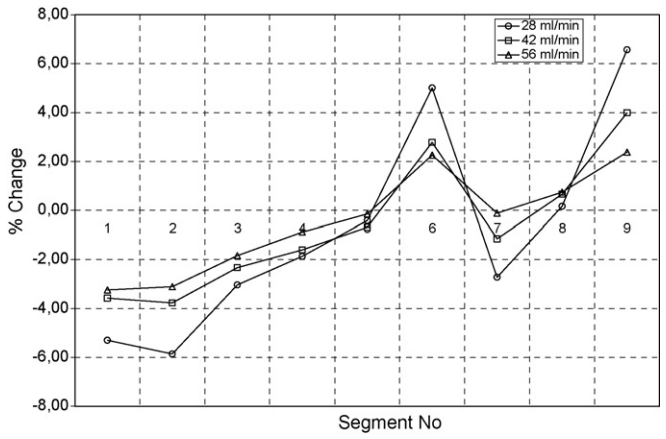

Fig. 7. The change in current density at 1 M methanol with a flow rate of 98 l min^{-1} to (a) 28 l min^{-1}, (b) 42 l min^{-1} and (c) 56 l min^{-1} at 70 °C.
vspace*6pt

at the methanol inlet (segment 8) and the minimum value was 39 mA cm^{-2} at the outlet of methanol (segment 1). When 0.5 M methanol is fed and 8 A current is withdrawn from the system, the current density distribution was as given in Fig. 6. There is a greater difference between current densities with respect to the current densities obtained with 1 M methanol feeding, that is the current density was 101 mA cm^{-2} (segment 9) and it was only 20 mA cm^{-2} (segment 1). For both 0.5 M and 1 M, the maximum current density was measured at the methanol inlet (segment 9) whereas the minimum current density was measured at the methanol outlet (segment 1). As the methanol is used on the path from methanol inlet (segment 9) through methanol outlet (segment 1), the current density decreases through methanol outlet (segment 1). For the same reason, the difference between the current densities at the methanol inlet and outlet increases as the methanol concentration decreases from 1 to 0.5 M.

The methanol flow rate was dropped from 98 to 28 ml min^{-1}, then from 98 to 42 ml min^{-1}, and at last from 98 to 56 ml min^{-1} to observe the effect of the methanol flow rate on the current density. The changes in current densities of segments are given in Figs. 7 and 8. For both 0.5 and 1 M methanol feeding, the highest deviation from the current densities measured at 98 ml min^{-1} was obtained at 28 ml min^{-1}. As the methanol flow rate decreases, the homogeneity of the current density distribution disappears and deviations increases.

3.2. Current density measurement at a constant oxygen flow rate (2.75 l min^{-1}) by alternating methanol flow rate

Next, the same measurements given in Section 3.1 were repeated by using oxygen instead of air. When 1 M methanol was fed at a flow rate of 98 ml min^{-1} and 8 A current was withdrawn from the system, the maximum current density acquired from the segments is 88 mA cm^{-2} (segment 9) while the minimum current density acquired is 34 mA cm^{-2} (segment 1) as seen in Fig. 9. When the concentration was decreased to 0.5 M, the difference between the current densities of the segments got higher (maximum current density was 99 mA cm^{-2} at segment 9 whereas minimum current density is 20 mA cm^{-2} at segment 1) (Fig. 10).

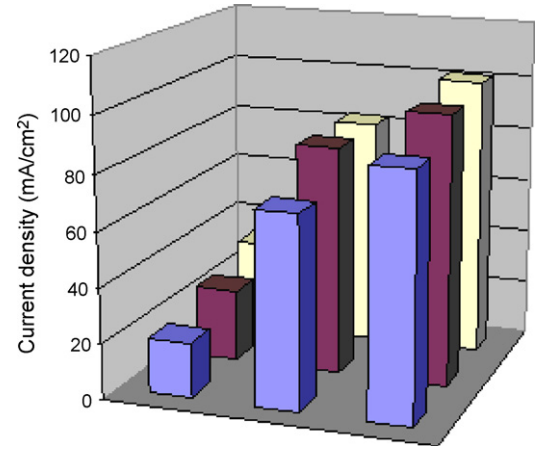

Fig. 6. Current density distribution for 98 l min^{-1} 0.5 M methanol flow rate, 13 l min^{-1} air flow rate and 8 A current.

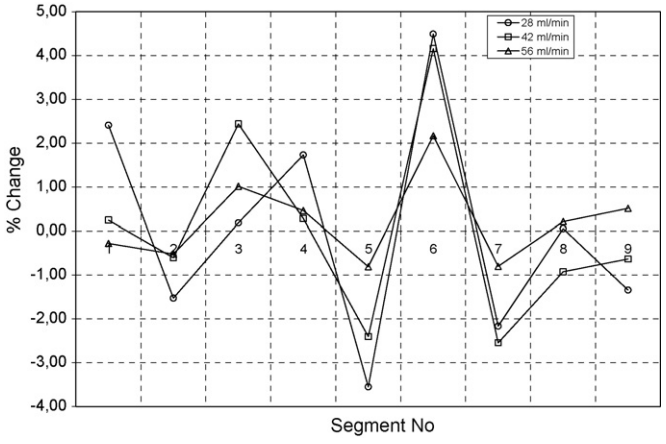

Fig. 8. The change in current density at 0.5 M methanol with a flow rate of 98 l min^{-1} to (a) 28 l min^{-1}, (b) 42 l min^{-1} and (c) 56 l min^{-1} at 70 °C.

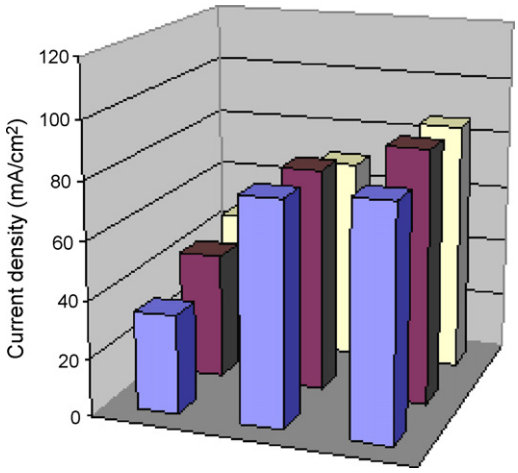

Fig. 9. Current density distribution for 98 l min^{-1} 1 M methanol flow rate, 2.75 l min^{-1} oxygen flow rate, 8 A current.

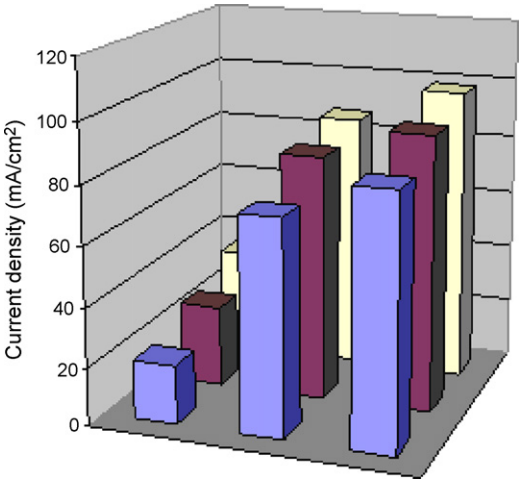

Fig. 10. DMFC current density distribution for 98 l min^{-1} 0.5 M methanol flow rate, 2.75 l min^{-1} oxygen flow rate, 8 A current.

The changes in current densities of segments are given in Figs. 11 and 12 for 1 and 0.5 M methanol, respectively. For both 0.5 and 1 M methanol feeding, the highest deviation from the current densities measured at 98 ml min^{-1} was obtained at 28 ml min^{-1} as in Section 3.1.

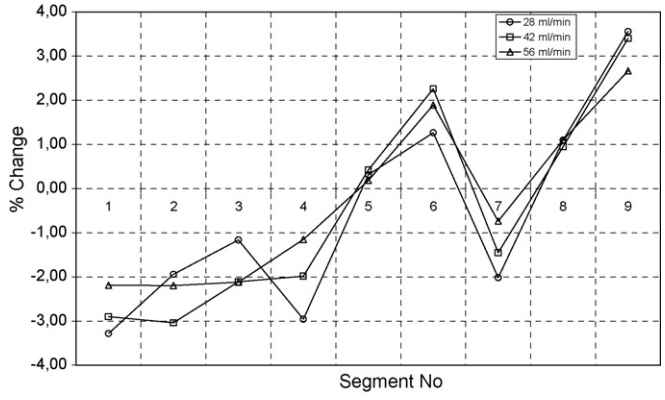

Fig. 11. Oxygen flow rate: 2.75 l min^{-1}; methanol flow rate: from 98 l min^{-1} (1 M) to (a) 28 l min^{-1}, (b) 42 l min^{-1} and (c) 56 l min^{-1}.

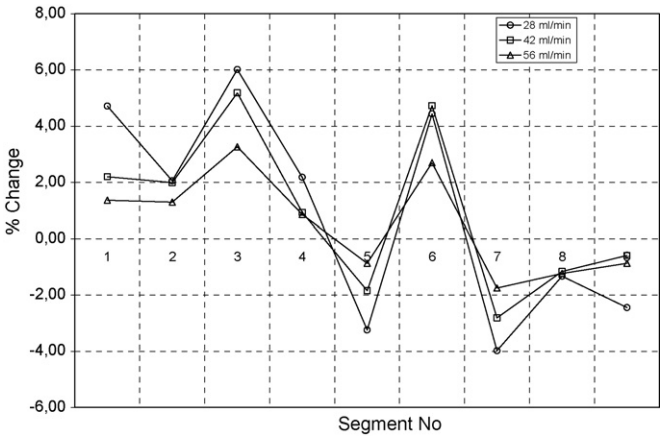

Fig. 12. Oxygen flow rate: 2.75 l min^{-1}; methanol flow rate: from 98 l min^{-1} (0.5 M) to (a) 28 l min^{-1}, (b) 42 l min^{-1} and (c) 56 l min^{-1}.

3.3. Current density measurement at a constant methanol flow rate (98 l min^{-1}) by alternating air flow rate

At this step, the aim of the experiments is to observe the effect of the air flow rate on the current density. When 1 M methanol was fed at a flow rate of 98 ml min^{-1} and 8 A current was withdrawn from the system, the current density distribution was as given in Fig. 13; it varies between 91 (segment 9) and 26 mA cm^{-2} (segment 1). When methanol concentration was decreased to 0.5 M, the maximum current density acquired from the segments is 105 mA cm^{-2} (segment 9) while the minimum current density acquired is 18 mA cm^{-2} (segment 1) as seen in Fig. 14.

Next, the air flow rate was decreased from 25 to 1.63 l min^{-1}, from 25 to 3.25 l min^{-1} and from 25 to 6.5 l min^{-1} at a constant methanol flow rate of 98 l min^{-1}, respectively. The maximum variation was obtained when the flow rate dropped from 25 to 1.63 l min^{-1} at the segment 2. The changes in current densities of segments are given in Figs. 15 and 16. For both 0.5 and 1 M methanol feeding, the highest deviation from the current density values measured at 25 l min^{-1} was obtained at 1.63 l min^{-1}.

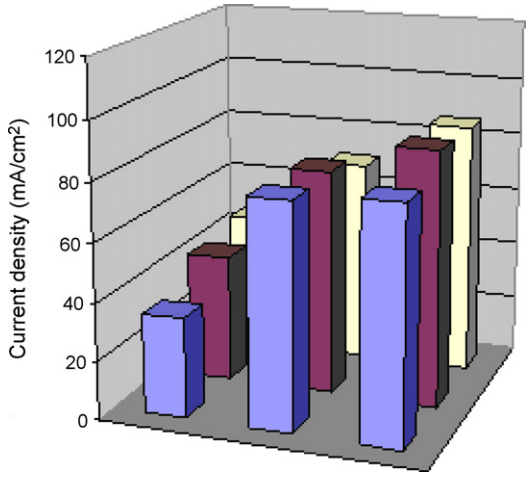

Fig. 13. Current density distribution for 98 l min^{-1} 1 M methanol flow rate, 25 l min^{-1} air flow rate, 8 A current.

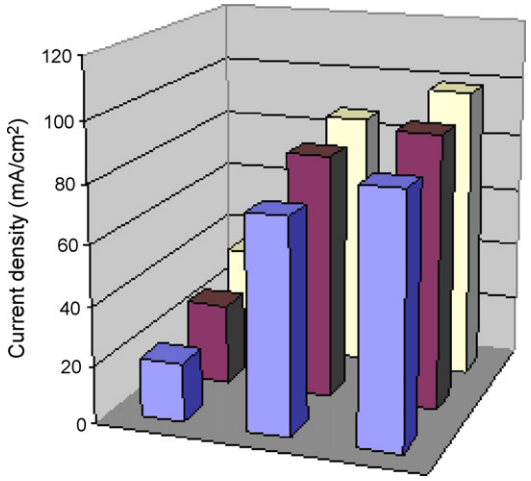

Fig. 14. Current density distribution (98 l min^{-1} 0.5 M methanol flow rate, 25 l min^{-1} air flow rate, 8 A current).

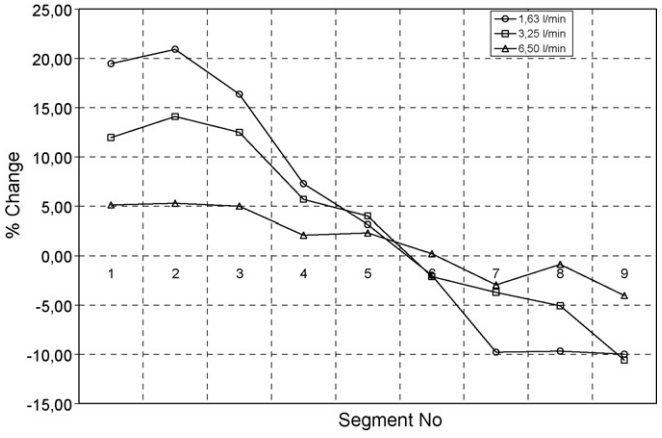

Fig. 15. Methanol flow rate: 98 l min^{-1} (1 M); air flow rate from 25 l min^{-1} to (a) 1.63 l min^{-1}, (b) 3.25 l min^{-1} and (c) 6.5 l min^{-1}.

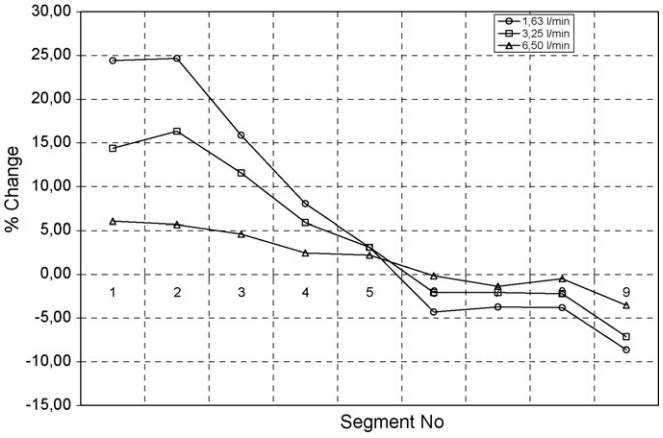

Fig. 16. Methanol flow rate: 98 ml min^{-1} (0.5 M); air flow rate from 25 l min^{-1} to (a) 1.63 l min^{-1}, (b) 3.25 l min^{-1} and (c) 6.5 l min^{-1}.

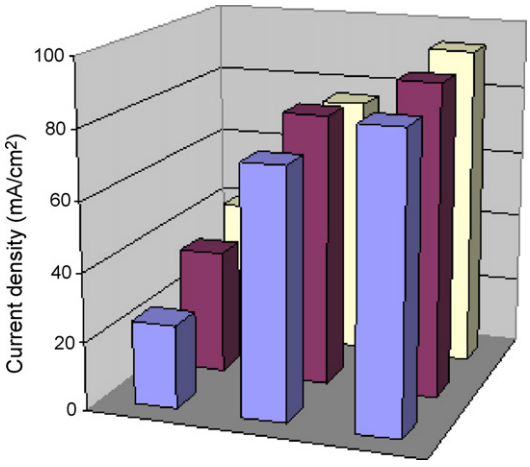

Fig. 17. Current density distribution (98 l min^{-1} 1 M methanol flow rate, 5.3 l min^{-1} oxygen flow rate, 8 A current).

3.4. Current density measurement at a constant methanol flow rate (98 l min^{-1}) by alternating oxygen flow rate

At last, the same measurements given in Section 3.3 were repeated by using oxygen instead of air. The current density distributions at 1 and 0.5 M methanol feeding were given in Figs. 17 and 18. When 1 M Methanol was fed at a flow rate of 98 ml min^{-1} and 8 A current was withdrawn from the system, the maximum current that has been withdrawn from the system was 94 mA cm^{-2} (segment 9) whereas the minimum was 24 mA cm^{-2} (segment 1). When the concentration is decreased to 0.5 M, the maximum current that has been withdrawn from the system was 106 mA cm^{-2} (segment 9) whereas the minimum was 17 mA cm^{-2} (segment 1).

Oxygen Flow Rate was decreased from 5.3 to 0.30 l min^{-1}, from 5.3 to 0.61 l min^{-1} and from 5.3 to 1.21 l min^{-1}. The maximum variation was obtained when the flow rate dropped from 5.3 to 0.30 l min^{-1}. The changes in current densities of segments are given in Figs. 19 and 20. For both 0.5 and 1 M methanol feeding, the highest deviation from the current density values measured at 5.3 l min^{-1} was obtained at 0.30 l min^{-1}.

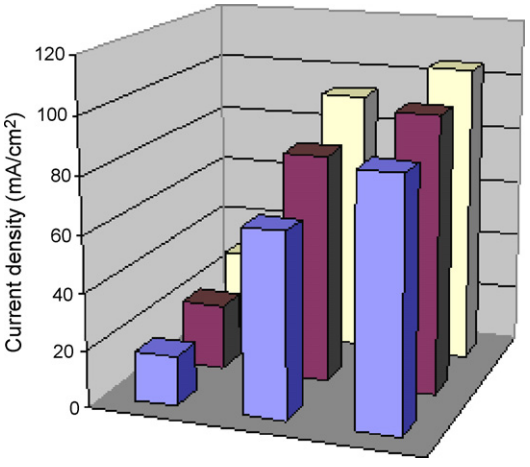

Fig. 18. Current density distribution (98 ml min^{-1} 0.5 M methanol flow rate, 5.3 l min^{-1} oxygen flow rate, 8 A current).

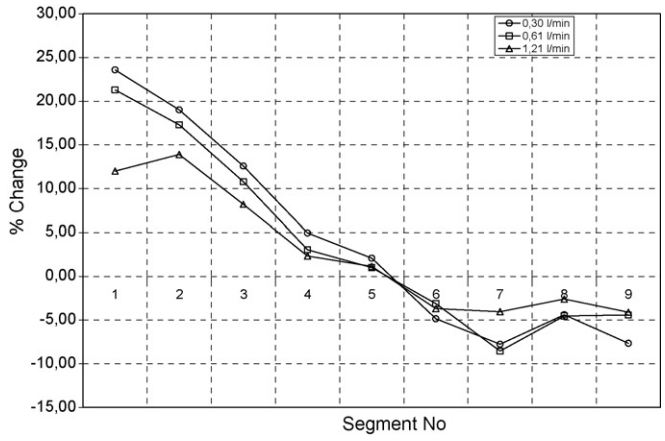

Fig. 19. Methanol flow rate: 98 ml min^{-1} (1 M); oxygen flow rate from 5.3 l min^{-1} to (a) 0.30 l min^{-1}, (b) 0.61 l min^{-1} and (c) 1.21 l min^{-1}.

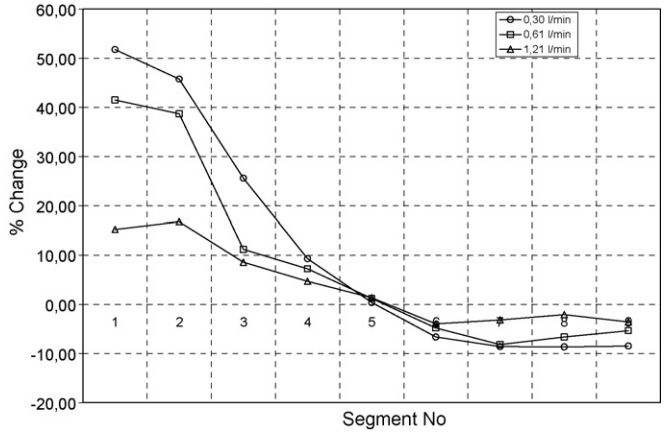

Fig. 20. Methanol flow rate: 98 ml min^{-1} (0.5 M); oxygen flow rate from 5.3 l min^{-1} to (a) 0.30 l min^{-1}, (b) 0.61 l min^{-1} and (c) 1.21 l min^{-1}.

The current density distribution for the whole cell is also similar to the air used experiment. As the oxidant is mostly utilized at the oxidant inlet (segments 1–3), current density at the inlet segments were high whereas the current density at the oxidant outlet (segments 7–9) were low due to the oxidant scarcity at these segments. Therefore, the least affected segments are the middle ones (segments 4–6).

4. Conclusions

As current distribution is essential for the life-time and performance of fuel cells, a current distribution measurement system has been presented for DMFCs to study the effect of the different operating parameters such as molarity, flow rate and reactant gas on the current density distribution.

a. When the flow rate of oxidant (air or hydrogen) or methanol was changed, the most effected segments from the view of current density are the nearest segments to the inlet stream.
b. As it was expected, the higher changes in parameters, the higher changes in current densities of segments have been observed.
c. It was also noticed that the current density fluctuation between segments is more when oxygen instead air was used as oxidant.
d. As all experiments done at 70 °C, temperature at each segment is assumed as constant and 70 °C. For future studies, temperature of each segment will be also measured to investigate the temperature effect on the current distribution.
e. The cell design improvements (especially on the flow fields) based on the findings can be done for the future studies.

References

[1] B. Geiger, R. Eckl, A. Wokaun, G.G. Scherer, J. Electrochem. Soc. 151 (3) (2004) A394–A398.
[2] F. Ay, Current distribution measurement for polymer electrolyte membrane fuel cells and direct methanol fuel cells, MS Thesis, Gebze Institute of Technology, Physics Department, Gebze, Turkey, 2005.
[3] N. Rajalakshmi, M. Raja, K.S. Dhathathreyan, J. Power Sources 112 (2002) 331–336.
[4] T. Hottinen, M. Noponen, T. Mennola, O. Himanen, M. Mikkola, P. Lund, J. Appl. Electrochem. 33 (2003) 265–271.
[5] A. Hakenjos, K. Tüber, J.O. Schumacher, C. Hebling, Fuel Cells 4 (3) (2004).
[6] S.J.C. Cleghorn, C.R. Derouin, M.S. Wilson, S. Gottesfeld, J. Appl. Electrochem. 28 (1998) 663–672.
[7] M.M. Mench, C.Y. Wang, M. Ishikawa, J. Electrochem. Soc. 150 (2003) A1052–A1059.
[8] J. Stumper, S.A. Campbell, D.P. Wilkinson, M.C. Johnson, M. Davis, Electrochim. Acta 43 (24) (1998) 3773–3783.